Computers and Mathematics with Applications 74 (2017) 2341–2347

Contents lists available at ScienceDirect

Computers and Mathematics with Applications

journal homepage: www.elsevier.com/locate/camwa

Breather, lump and X soliton solutions to nonlocal KP equation☆

Xiaoen Zhang [a], Yong Chen [a,b,*], Yong Zhang [c]

[a] Shanghai Key Laboratory of Trustworthy Computing, East China Normal University, Shanghai, 200062, China
[b] Department of Physics, Zhejiang Normal University, Jinhua 321004, China
[c] College of Mathematics and Systems Science, Shandong University of Science and Technology, Qingdao, 266590, China

ARTICLE INFO

Article history:
Received 15 April 2017
Received in revised form 16 June 2017
Accepted 5 July 2017
Available online 1 August 2017

Keywords:
Nonlocal KP equation
Alice–Bob system
X soliton
Lump solution

ABSTRACT

Breather, lump and X soliton solutions are presented via the Hirota bilinear method, to the nonlocal (2+1)-dimensional KP equation, derived from the Alice–Bob system. The resulting breather contains two cases, one is the line breather and another is the normal breather, both of which are different from the solutions of the classical (2+1)-dimensional KP equation; the X soliton is found with the long wave limit by some constraints to the parameters; the lump solution is obtained in virtue of two methods, one is as the long wave limit of breather theoretically, the other is with the quadratic function method, which can be guaranteed rationally localized in all directions in the space under some constraints of the parameters. By choosing specific values of the involved parameters, the dynamic properties of some breather, lump solutions to nonlocal KP equation are plotted, as illustrative examples.

1. Introduction

Generally speaking, many non-Hermitian systems with parity-time (PT) symmetry [1] have been studied due to its supernatural physics properties, especially in the optics [2,3]. This concept originated from the theory of quantum fields and brought about new strategies in achieving a harmonic interaction between optical gain and loss. Here the parity reflection operator $\mathcal{P}$: $p \to -p, x \to -x$, is the linear and the time reflection operator $\mathcal{T}$: $p \to -p, t \to -t, i \to -i$ is anti-linear [4]. In [5], Yang et al. investigated the nonlinear wave propagation in parity-time symmetric localized potentials. Usually, a necessary condition to PT symmetry is that its complex refractive satisfies a basic condition $V(-x) = V^*(x)$ so as to manifest the real part of V is symmetric and the imaginary component is antisymmetric. As to multidimensions, the PT symmetry has been extended to the partial-parity-time (PPT) symmetry [6]. Up to now, there are many articles referred to the PT symmetry and PPT symmetry, such as the integrable nonlocal nonlinear Schrödinger equation (NLS) [7,8], which has been proved that it has an infinite number of conservation laws via the inverse scattering method, whereafter based on the general AKNS scattering problems [9], a series of new nonlocal nonlinear integrable equations are derived, such as modified Korteweg–de Vries (mKdV), sine-Gordon, $(1+1)$ and $(2+1)$ dimensional three-wave interaction, derivative NLS, Davey–Stewartson (DS) equations.

Recently, Lou [10,11] put forward an Alice–Bob system, in which, the event A can be regarded as the decrease of ice at Arctic sea in the summer of 2007 and the event B can be considered to be responsible for the heavy freezing rain in winter

☆ The project is supported by the Global Change Research Program of China (No. 2015CB953904), National Natural Science Foundation of China (No. 11675054, 11435005). and Shanghai Collaborative Innovation Center of Trustworthy Software for Internet of Things (No. ZF1213).

* Corresponding author at: Shanghai Key Laboratory of Trustworthy Computing, East China Normal University, Shanghai, 200062, China.
E-mail address: ychen@sei.ecnu.edu.cn (Y. Chen).

http://dx.doi.org/10.1016/j.camwa.2017.07.004
0898-1221/

2008 in Southern, moreover the strong El Nino event occurred in 1997 and the heavy Yangtze River flooding in 1998 can also be described with the Alice–Bob system. Meanwhile, it is reported that the detection of the signal of gravitational wave (can be called the event B) is closely related to the event A, which can be regarded as the merging of two black holes from 1.3 billion light years away. These two far-away particles Alice and Bob may be entangled each other with a suitable operator $\hat{f}$, that is

$$B(x', t') = \hat{f}A = A^f, \tag{1}$$

where $\hat{f}$ indicates the shifted parity ($\hat{P}_s$) transformation for the spatial and the delayed time reversal ($\hat{T}_d$) for the time variable

$$x' = -x + x_0 \equiv \hat{P}_s x, \qquad t' = -t + t_0 \equiv \hat{T}_d t, \tag{2}$$

if $x_0 = 0$, $t_0 = 0$, then it can be reduced the general PT symmetry, the model with $x_0 = 0$ has been studied by many authors, but it is a new model for $x_0 \neq 0$.

As to classical KP equation, the lump solution [12], rogue wave [13,14] are presented via the bilinear method. Meanwhile, some rational solutions to other equations are obtained, such as the Schrödinger equations [15], Shallow-Water equation [16], the Yajima–Oikawa systems [17], $(3+1)$-dimensional Jimbo–Miwa equation [18,19], KP-Boussinesq equation [20], KP-like equation [21], Hirota–Satsuma-like equation [22], and other Hirota bilinear equation [23–25]. Some of these rational solutions can be described the Rossby solitary [26] wave in the ocean. Especially, a special rational solution (X soliton) [27] attracts a lot of attentions. However, there are only several nonlocal equations whose solutions are given, for example, the rational solutions to nonlocal DSI [28,29], DSII equations [30] and the multi-soliton to Alice–Bob system [10].

In this paper, we discuss the dynamics properties to two kinds of nonlocal KP equations derived from the nonlocal Alice–Bob system, one is the nonlocal KPI equation and the other is KPII equation. Firstly, we give the line breather to these two nonlocal KP equations, compared with the classical line breather, this kind of line breather is composed with the aggregation of some parallel line wave. Thereafter, by a long wave limit, two unexpected phenomena appear, one is the lump solution and the other is the interaction between two solitons. It is interesting that the evolutionary two-soliton dynamics behavior to the nonlocal KPI equation is similar to a progress of the phase of the moon, that is, it appears a first quarter in the beginning, changes into a full moon and reduces to a last quarter in the end. While the interaction between the two-soliton to nonlocal KPII equation is different, it begins with a symmetric two-soliton about the y axis, then it divides into a X soliton and this X soliton is symmetric not only about the y axis but also with the x axis, after the fusion, it returns back to two solitons. Furthermore, we study the lump solution to nonlocal KPI equation via the quadratic function method, discuss the different dynamical behaviors caused by the effect of x_0, y_0 to the lump solution and give the comparison figures with different x_0, y_0.

The outline of this paper is as follows: in Section 2, the two classes of nonlocal KP equations are introduced and their multi-soliton solutions are given. Then the breather, lump, X soliton solutions to KPI equation and the breather, X soliton solutions to KPII equation are presented in Section 3. In Section 4, via another method (quadratic function method), the lump solution to nonlocal KPI equation is obtained. Some conclusion and summary are given in Section 4.

2. Nonlocal KPI and KPII equations

Based on the Alice–Bob referred in [10], the nonlocal KPI equation and KPII equations are derived as

$$A_{xt} + \left(A_{xx} + 3AB + \frac{3}{2}A^2 - \frac{3}{2}B^2\right)_{xx} - A_{yy} = 0, \tag{3a}$$

$$A_{xt} + \left(A_{xx} + 3AB + \frac{3}{2}A^2 - \frac{3}{2}B^2\right)_{xx} + A_{yy} = 0, \tag{3b}$$

where $B = A^f$, and A^f represents three cases:

$$A^f = \hat{P}_s^{xy}\hat{T}_d A = A(-x + x_0, -y + y_0, -t + t_0),$$
$$A^f = \hat{P}_s^{x}\hat{T}_d A = A(-x + x_0, y, -t + t_0),$$
$$A^f = \hat{P}_s^{y} dA = A(x, -y + y_0, t),$$

Eqs. (3a) and (3b) can be changed into the following bilinear form respectively

$$D_t D_x g \cdot g + D_x^4 g \cdot g - D_y^2 g \cdot g = 0, \tag{4a}$$

$$D_t D_x g \cdot g + D_x^4 g \cdot g + D_y^2 g \cdot g = 0, \tag{4b}$$

under the transformation $A = B = 2(\ln g)_{xx}$ and g satisfies $g(x, y, t) = g(-x + x_0, -y + y_0, -t + t_0)$.

The multi-solitons of this nonlocal KPI can be written as

$$g = \sum_{\nu=1,-1} K_\nu \cosh\left(\frac{1}{2}\sum_{j=1}^{N} \nu_j \eta_j\right), \tag{5}$$

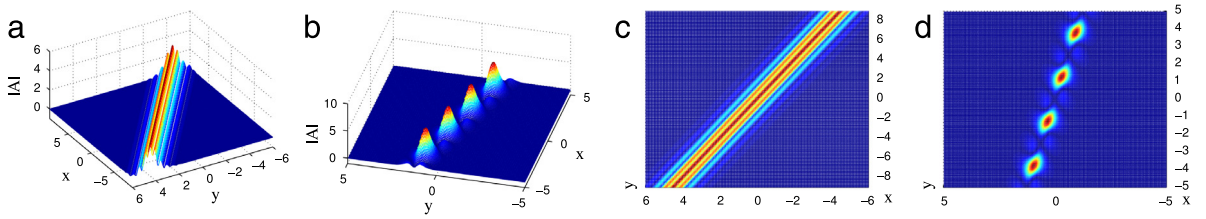

Fig. 1. The breather to corresponding $|A|$ determined by Eq. (5) when $N = 2$, (a) is the line breather by choosing $k_1 = 1+3I$, $k_2 = 1-3I$, $p_1 = p_2 = 2$, $x_0 = 0$, $t_0 = 0$, $y_0 = 0$, $\eta_1^0 = \eta_2^{0*} = 0$, (b) is the normal breather by choosing $k_1 = 1+2I$, $k_2 = 1-2I$, $p_1 = -2I$, $p_2 = 2I$, $t_0 = 0$, $y_0 = 0$, $x_0 = 0$, $\eta_1^0 = 0$, $\eta_2^0 = 0$, (c) and (d) are the corresponding density plots to (a) and (c) respectively.

where

$$\eta_j = k_j\left[\left(x - \frac{x_0}{2}\right) + p_j\left(y - \frac{y_0}{2}\right) - (k_j^2 - p_j^2)\left(t - \frac{t_0}{2}\right)\right] + \eta_j^0,$$
$$K_\nu = \prod_{i>j}\sqrt{3(k_i - \nu_i\nu_j k_j)^2 + (p_i - p_j)^2},$$
$$\nu_i = 1, -1, \quad (i = 1, 2, \ldots, N).$$

Similarly, the muiti-solitons to KPII equation are derived as

$$g = \sum_{\nu=1,-1} K_\nu \cosh\left(\frac{1}{2}\sum_{j=1}^{N}\nu_j\eta_j\right), \tag{6}$$

where

$$\eta_j = k_j\left[\left(x - \frac{x_0}{2}\right) + p_j\left(y - \frac{y_0}{2}\right) - (k_j^2 + p_j^2)\left(t - \frac{t_0}{2}\right)\right] + \eta_j^0,$$
$$K_\nu = \prod_{i>j}\sqrt{3(k_i - \nu_i\nu_j k_j)^2 - (p_i - p_j)^2},$$
$$\nu_i = 1, -1, \quad (i = 1, 2, \ldots, N).$$

In earlier works, by some constraints to the parameters on the two-soliton, a family of analytical breathers solutions can be obtained. Inspired by the general technique, we give the line breather to Eq. (5) when $N = 2$ by setting

$$k_1 = 1 + 3I, \qquad k_2 = 1 - 3I, \qquad p_1 = p_2 = 2, \qquad x_0 = 0, \qquad t_0 = 0, \qquad y_0 = 0, \qquad \eta_1^0 = \eta_2^{0*} = 0,$$

then g can be written as

$$g = 4\sqrt{3}(3I\cosh(30t + x + 2y) + \cos(30t + 3x + 6y)). \tag{7}$$

The corresponding solutions $|A|$ in the (x, y) plane are shown in Fig. 1. Compared with the classical line wave, which keeps in parallel state and out of interaction with each other, this kind of line wave is composed with many line waves and they gather together, merge into one line wave, we can call this line wave as the line breather. Moreover, by choosing different parameters, such as $k_1 = 1 + 2I$, $k_2 = 1 - 2I$, $p_1 = -2I$, $p_2 = 2I$, $t_0 = 0$, $y_0 = 0$, $x_0 = 0$, $\eta_1^0 = 0$, $\eta_2^0 = 0$, then g can be written as

$$g = 4I(4\cosh(7t + 4y + x) + \cos(6t - 2x + 2y)) \tag{8}$$

and the corresponding $|A|$ in the (x, y) changes into the normal breathers, which is shown in Fig. 1.

Based on the idea of getting the breather to the nonlocal KPI equation, we present the line breather and the normal breather to the nonlocal KPII equation, whose characters are similar to the corresponding KPI equation, it is shown in Fig. 2 respectively.

Based on the idea to the generate the lump solution for the general equations, we obtain the lump solution to the nonlocal KPI equation by taking a long wave limit to the general two-soliton solution. Putting

$$k_1 = l_1\varepsilon, \qquad k_2 = l_2\varepsilon, \qquad \eta_1^0 = I\pi, \qquad \eta_2^0 = -I\pi, \tag{9}$$

in Eq. (5) when $N = 2$ and setting the limit $\varepsilon = 0$, then the function g can be changed into

$$g = \frac{\sqrt{(p_2 - p_1)^2}}{4}l_1 l_2(\omega_1\omega_2 + \omega_0), \tag{10}$$

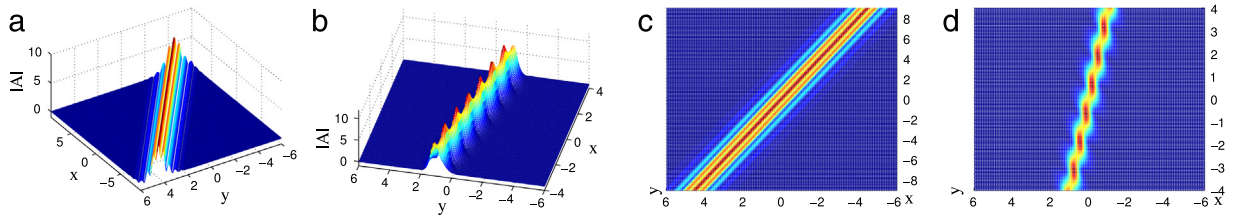

Fig. 2. The breather to corresponding KPII equation, (a) is the line breather, (b) is the normal breather, (c) and (d) are the corresponding density plots to (a) and (c) respectively by choosing the same parameters.

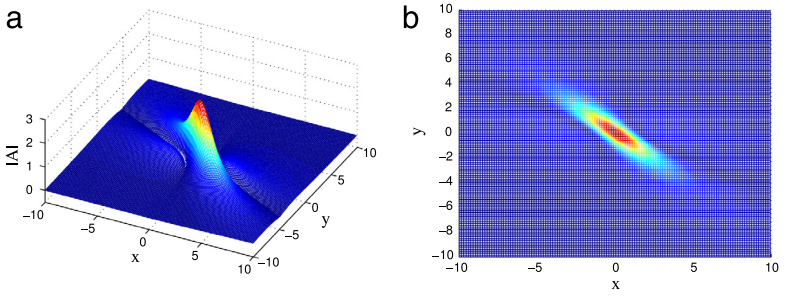

Fig. 3. The lump solution to Eq. (12) by choosing $p_1 = 1 + I$, $p_2 = 1 - I$, $x_0 = 0$, $y_0 = 0$, $t_0 = 0$, (a) is the 3D plot, (b) is the corresponding density plot.

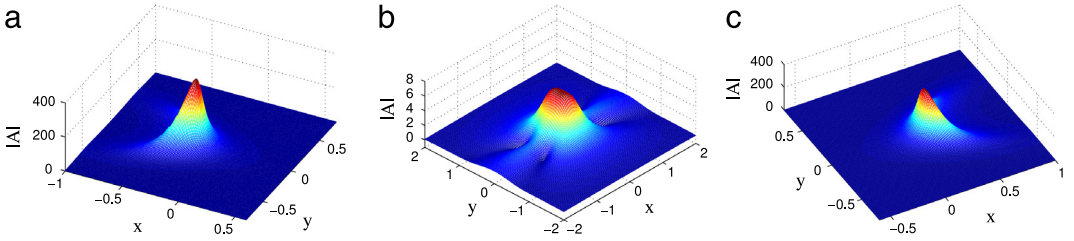

Fig. 4. The evolution plots to the interaction of two-soliton by choosing $p_1 = 0.9 - 2I$, $p_2 = -0.9 + 2I$, $x_0 = 0$, $y_0 = 0$, $t_0 = 0$, at times (a) $t = -0.18$, (b) $t = 0$, (c) $t = 0.18$.

where

$$\begin{aligned} \omega_1 &= 2x - x_0 + (2y - y_0)p_1 + (2t - t_0)p_1^2, \\ \omega_2 &= 2x - x_0 + (2y - y_0)p_2 + (2t - t_0)p_2^2, \\ \omega_0 &= -\frac{12}{(p_1 - p_2)^2}. \end{aligned} \tag{11}$$

Then the rational solution of $|A|$ can be written as

$$|A| = \left| -\frac{8(\omega_1^2 + \omega_2^2 - 2\omega_0)}{(\omega_1\omega_2 + \omega_0)^2} \right|. \tag{12}$$

Setting the parameter constraint $p_2 = p_1^*$ can guarantee the solution $|A|$ in Eq. (12) is nonsingular. Then the lump solution can be obtained by choosing $p_1 = a_1 + b_1 I$, $p_2 = a_1 - b_1 I$ and the solution $|A|$ in Eq. (12) is a constant along a trajectory determined by $[x(t), y(t)]$,

$$\begin{aligned} &2x - x_0 + a(2y - y_0) + (a^2 - b^2)(2t - t_0) = 0, \\ &b(2y - y_0) + 2ab(2t - t_0) = 0. \end{aligned} \tag{13}$$

Furthermore, when (x, y) goes to infinity, the corresponding $|A|$ will approach to 0 when t is an arbitrary value, whose dynamical behavior is shown in Fig. 3.

In addition, when $p_2 = -p_1 = a_2 + b_2 I$, then $a_2 < b_2$ can guarantee Eq. (12) is nonsingular. Now another interesting interaction between two-soliton solutions is depicted in Fig. 4.

It is obvious that the two-solitons are parabolic solitary and they are symmetric about y direction, similar to a crescent moon, as time goes on, these two parabolic solitary decompose into a full moon and their amplitude is lower than any other

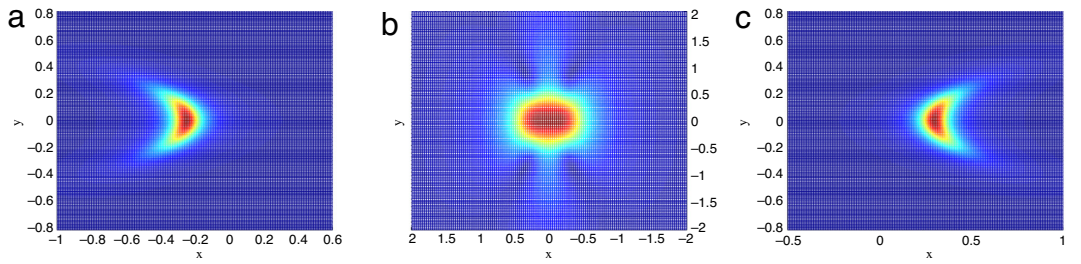

Fig. 5. The corresponding density plots to Fig. 4.

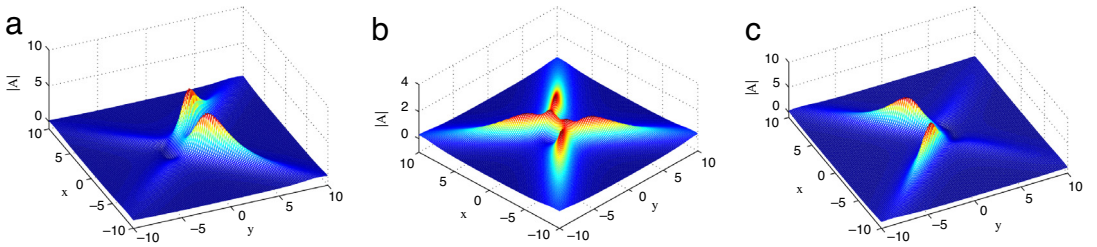

Fig. 6. The evolution plots to the interaction of two-soliton by choosing $p_1 = 1 - 0.25I$, $p_2 = -1 + 0.25I$, $x_0 = 0$, $y_0 = 0$, $t_0 = 0$, at times (a) $t = -1$, (b) $t = 0$, (c) $t = 1$.

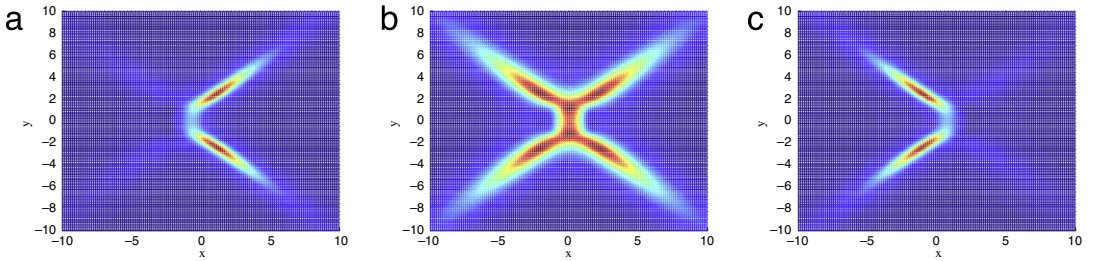

Fig. 7. The corresponding density plots of Fig. 6.

time, after the decomposition, they continue to move with the same speed, which can also be called a progress from the first quarter to the last quarter, its corresponding density plots are shown in Fig. 5.

Furthermore, taking the long wave limit to the breather, the evolution plots of two-soliton to nonlocal KPII equation are depicted in Fig. 6 with the parameters $p_2 = -p_1 = a_3 + b_3 I$. In this case we must set $a_3 > b_3$ in order to guarantee the corresponding solution is nonsingular.

It can be seen that this kind of solution is still symmetric about y direction, and they will decompose into a X soliton when $t = 0$, whose amplitude is lower than any time. This progress can be called the mechanism of X soliton aroused by two parabolic solitary. Similar to the KPI equation, this progress is also an elastic collision, its corresponding density plots are shown in Fig. 7.

But it is a pity that we cannot find the lump solution to nonlocal KPII equation, the solution $|A|$ cannot be guaranteed nonsingular no matter what the values of the parameters p_1 and p_2.

3. Lump solution to nonlocal KPI equation

Section 2 has given the lump solution to nonlocal KPI equation with the long wave limit to the breather, this section, we want to present the lump solution by using the positive quadratic function, assume g as

$$g = m^2 + n^2 + a_7, \tag{14}$$

where

$$m = a_1\left(x - \frac{x_0}{2}\right) + a_2\left(y - \frac{y_0}{2}\right) + a_3\left(t - \frac{t_0}{2}\right), \tag{15a}$$

$$n = a_4\left(x - \frac{x_0}{2}\right) + a_5\left(y - \frac{y_0}{2}\right) + a_6\left(t - \frac{t_0}{2}\right), \tag{15b}$$

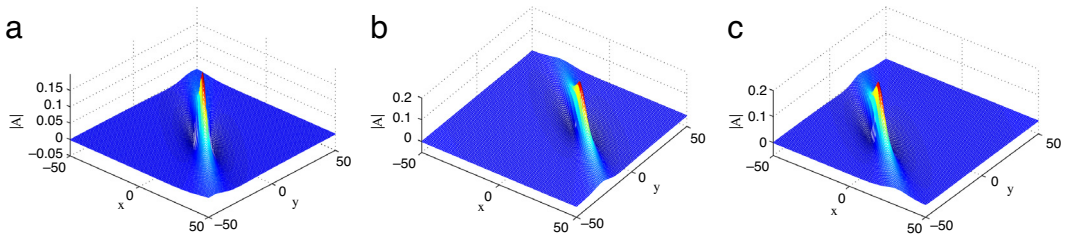

Fig. 8. Three kinds of lump solutions with different x_0 and y_0, (a) by choosing $a_1 = 0.6, a_2 = 1, a_4 = 1, a_5 = 0.8, x_0 = -20, y_0 = -20, t = 0, t_0 = 0$, (b) by choosing $a_1 = 0.6, a_2 = 1, a_4 = 1, a_5 = 0.8, x_0 = 0, y_0 = 0, t = 0, t_0 = 0$, (c) by choosing $a_1 = 0.6, a_2 = 1, a_4 = 1, a_5 = 0.8, x_0 = 20, y_0 = 20, t = 0, t_0 = 0$.

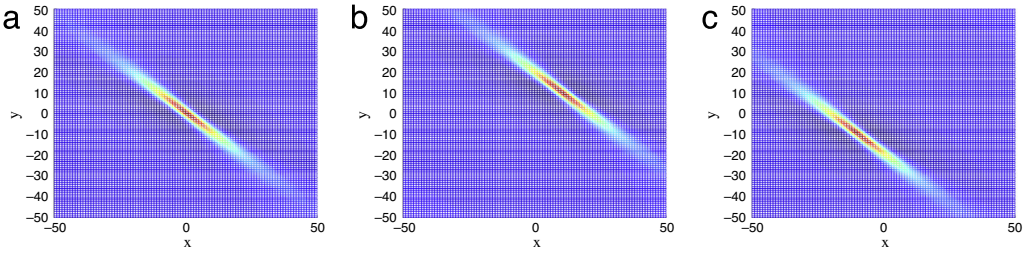

Fig. 9. The corresponding density plots of Fig. 8.

where $a_i (1 \leq i \leq 7)$ are real parameters to be determined. A direct Maple symbolic calculation to g can generate the following constraint equation

$$a_3 = \frac{a_1 a_2^2 - a_1 a_5^2 + 2a_2 a_4 a_5}{a_1^2 + a_4^2}, \qquad a_6 = \frac{a_4 a_5^2 - a_4 a_2^2 + 2a_1 a_2 a_5}{a_1^2 + a_4^2}, \qquad a_7 = \frac{3(a_1^6 + 3a_1^4 a_4^2 + 3a_1^2 a_4^4 + a_4^6)}{(a_1 a_5 - a_2 a_4)^2}, \tag{16}$$

which should be satisfied $a_1 a_5 - a_2 a_4 \neq 0$, then the corresponding solution $|A|$ can be written as

$$|A| = \left| \frac{4(a_1^2 + a_4^2)g - 8(a_1 m + a_4 n)^2}{g^2} \right| \tag{17}$$

where g, m, n are determined by Eqs. (15a), (15b) and (14). In this class of lump solutions, 4 parameters are arbitrary provided that $a_i (1 \leq i \leq 7)$ satisfy $a_1 a_5 - a_2 a_4 \neq 0$. It is observed that when (x, y) goes to infinity, the corresponding solution $|A|$ still goes to 0, whose dynamical character is shown in Fig. 8. It is important to emphasize the characters of this class of lump solutions are similar to the lump solution given by the long wave limit of breather.

In Fig. 8, we can know that the location of lump soliton will be changed due to the different values of x_0, y_0, which can also be regarded as the evolution plots, that is, as the time goes, Fig. 8(a) may be turn into Fig. 8(b) and (c). Therefore, the values of x_0 and y_0 play an important role to the evolution character. Its corresponding density plots are depicted in Fig. 9.

4. Conclusion

In this paper, the line breather and period normal breather to the nonlocal KPI and KPII equations are obtained by the bilinear transformation and demonstrated by 3D figures. Especially, these obtained line breathers are composed by a series of parallel line waves and these line waves are merged into together, which are different from the classical KP equation. Furthermore, the lump solution to nonlocal KPI equation is given by using two methods, localized analytical solution in rational form. Then we discuss the influence of x_0 and y_0 to the character of the lump solution. Apart from that, an interesting interaction between two-soliton is found, this phenomena is symmetric about the y direction and will decompose into a X soliton when $t = 0$, its energy becomes less than any other time accordingly, which can be regarded as the formation mechanism of the X soliton. However, it is a pity that we cannot find the rogue wave to these nonlocal KPI and KPII equations, no matter it is line rogue wave or localized 2D rogue wave. In our further work, maybe we can use other methods to get the rogue wave and discuss more dynamics properties to these nonlocal KP equations, in addition, based on the theory of the classical integrable system [31,32] we can study these Hamiltonian structures of these nonlocal equations.

Acknowledgments

We would like to express our sincere thanks to S.Y. Lou, W.X. Ma, E.G. Fan, Z.Y. Yan, Y.H. Wang, J.C. Chen and other members of our discussion group for their valuable comments.

References

[1] C.M. Bender, S. Boettcher, Real spectra in non-hermitian hamiltonians having *PT* symmetry, Phys. Rev. Lett. 80 (1998) 5243–5246. http://dx.doi.org/10.1103/PhysRevLett.80.5243.

[2] K.G. Makris, R. El-Ganainy, D.N. Christodoulides, Beam dynamics in *PT* symmetric optical lattices, Phys. Rev. Lett. 100 (2008) 103904. http://dx.doi.org/10.1103/PhysRevLett.100.103904.

[3] A. Guo, G.J. Salamo, D. Duchesne, R. Morandotti, M.V. Ravat, V. Aimez, G.A. Siviloglou, D.N. Christodoulides, Observation of *PT*-symmetry breaking in complex optical potentials, Phys. Rev. Lett. 103 (2009) 093902. http://dx.doi.org/10.1103/PhysRevLett.103.093902.

[4] Z.Y. Yan, Integrable *PT*-symmetric local and nonlocal vector nonlinear Schrödinger equations: A unified two-parameter model, Appl. Math. Lett. 47 (2015) 61–68. http://dx.doi.org/10.1016/j.aml.2015.02.025.

[5] S. Nixon, J.K. Yang, Nonlinear wave dynamics near phase transition in *PT*-symmetric localized potentials, Physica D 331 (2016) 48–57. http://dx.doi.org/10.1016/j.physd.2016.05.006.

[6] J.K. Yang, Symmetry breaking of solitons in two-dimensional complex potentials, Phys. Rev. E 91 (2015) 023201. http://dx.doi.org/10.1103/PhysRevE.91.023201.

[7] A.S. Fokas, Integrable multidimensional versions of the nonlocal nonlinear Schrödinger equation, Nonlinearity 29 (2016) 319–324. http://dx.doi.org/10.1088/0951-7715/29/2/319.

[8] M.J. Ablowita, Z.H. Musslimani, Integrable Nonlocal Nonlinear Schroödinger Equation, Phys. Rev. Lett. 110 (2013) 064105. http://dx.doi.org/10.1103/PhysRevLett.110.064105.

[9] M.J. Ablowita, Z.H. Musslimani, Integrable nonlocal nonlinear equation, Stud. Appl. Math. (2016). http://dx.doi.org/10.1111/sapm.12153.

[10] S.Y. Lou, Alice-Bob systems, $P_s - T_d - C$ principles and multi-soliton solutions, 2016. arXiv.Orgdoi: arXiv:1603.03975v2.

[11] S.Y. Lou, Alice-Bob physics: coherent solutions of nonlocal KdV systems, 2017. ArXiv.Orgdoi: arXiv:1606.03154v2.

[12] W.X. Ma, Lump solutions to the Kadomtsev-Petviashvili equation, Phys. Lett. A 379 (2015) 1975–1978. http://dx.doi.org/10.1016/j.physleta.2015.06.061.

[13] X.E. Zhang, Y. Chen, X.Y. Tang, Rogue wave and a pair of resonance stripe solitons to a reduced generalized (3+1)-dimensional KP equation, 2016. arXiv.Orgdoi: arXiv:1610.09507v1.

[14] C. Qian, J.G. Rao, Y.B. Liu, J.S. He, Rogue waves in the three-dimensional Kadomtsev-Petviashvili equation, Chin. Phys. Lett. 33 (2016) 110201. http://dx.doi.org/10.1088/0256-307X/33/11/110201.

[15] L.M. Ling, L.C. Zhao, B.L. Guo, Darboux transformation and multi-dark soliton for N-component nonlinear Schrödinger equations, Nonlinearity 28 (2015) 3243–3261. http://dx.doi.org/10.1088/0951-7715/28/9/3243.

[16] Y. Zhang, H.H. Dong, X.E. Zhang, H.W. Yang, Rational solutions and lump solutions to the generalized (3+1)-dimensional Shallow Water-like equation, Comput. Math. Appl. 73 (2017) 246–252. http://dx.doi.org/10.1016/j.camwa.2016.11.009.

[17] J.C. Chen, Y. Chen, B.F. Feng, K.I. Maruno, Rational solutions to two- and one–dimensional multicomponent Yajima-Oikawa systems, Phys. Lett. A 379 (2015) 1510–1519. http://dx.doi.org/10.1016/j.physleta.2015.02.040.

[18] X.E. Zhang, Y. Chen, Rogue wave and a pair of resonance stripe solitons to a reduced (3+1)-dimensional Jimbo-Miwa equation, Commun. Nonlinear Sci. Numer. Simul. (2017). http://dx.doi.org/10.1016/j.cnsns.2017.03.021.

[19] W.X. Ma, Lump-Type solutions to the (3+1)-dimensional Jimbo-Miwa equation, Int. J. Nonlinear Sci. Numer. Simul. 17 (2016) 355–359. http://dx.doi.org/10.1515/ijnsns-2015-0050.

[20] X. Lv, S.T. Chen, W.X. Ma, Constructing lump solutions to a generalized Kadomtsev-Petviashvili-Boussinesq equation, Nonlinear Dynam. 86 (2016) 523–534. http://dx.doi.org/10.1007/s11071-016-2905-z.

[21] X. Lv, W.X. Ma, Y. Zhou, C.M. Khalique, Rational solutions to an extended Kadomtsev-Petviashvili-like equation with symbolic computation, Comput. Math. Appl. 71 (2016) 1560–1567. http://dx.doi.org/10.1016/j.camwa.2016.02.017.

[22] X. Lv, W.X. Ma, S.T. Chen, C.M. Khalique, A note on rational solutions to a Hirota-Satsuma-like equation, Appl. Math. Lett. 58 (2016) 13–18. http://dx.doi.org/10.1016/j.aml.2015.12.019.

[23] W.X. Ma, Y. Zhou, R. Dougherty, Lump-type solutions to nonlinear differential equationsderived from generalized bilinear equations, Internat. J. Modern Phys. B 30 (2016) 1640018. http://dx.doi.org/10.1142/S021797921640018X.

[24] L.N. Gao, X.Y. Zhao, Y.Y. Zi, J. Yu, X. Lv, Resonant behavior of multiple wave solutions to a Hirota bilinear equation, Comput. Math. Appl. 72 (2016) 1225–1229. http://dx.doi.org/10.1016/j.camwa.2016.06.008.

[25] X. Lv, W.X. Ma, Study of lump dynamics based on a dimensionally reduced Hirota bilinear equation, Nonlinear Dynam. 85 (2016) 1217–1222. http://dx.doi.org/10.1007/s11071-016-2755-8.

[26] H.W. Yang, B.S. Yin, Y.L. Shi, Q.B. Wang, Forced ILW-Burgers equation as a model for rossby solitary waves generated by topography in finite depth fluids, J. Appl. Math. 2012 (2012) 491343. http://dx.doi.org/10.1155/2012/491343.

[27] F. Baronio, S. Wabnitz, S.H. Chen, M. Onorato, S. Trillo, Y. Kodama, Optical nonlinear dark x-waves, 2016. arXiv.Orgdoi: arXiv:1608.08771v1.

[28] J.G. Rao, Y. Cheng, J.S. He, Rational and semi-rational solutions to the *x*-nonlocal davey-stewartson i equation, 2016 ResearchGate. http://dx.doi.org/10.13140/RG.2.2.32850.35523.

[29] J.G. Rao, Y.S. Zhang, A.S. Fokas, J.S. He, Rogue waves of the nonlocal davey-stewartson i equation, 2017 ResearchGate. http://dx.doi.org/10.13140/RG.2.2.14395.41766.

[30] J.G. Rao, Y. Cheng, J.S. He, Rational and semi-rational solutions of the x-nonlocal and nonlocal davey-stewartson II equation, 2017 ResearchGate. http://dx.doi.org/10.13140/RG.2.2.33792.43528.

[31] X.Z. Wang, H.H. Dong, Y.X. Li, Some reductions from a Lax integrable system and their Hamiltonian structures, Appl. Math. Comput. 218 (2012) 10032–10039. http://dx.doi.org/10.1016/j.amc.2012.03.071.

[32] X.Y. Li, Q.L. Zhao, Y.X. Li, H.H. Dong, Binary Bargmann symmetry constraint associated with 3×3 discrete matrix spectral problem, J. Nonlinear Sci. Appl. 8 (2015) 496–506.